coatings

MDPI

Article

Stability of Polyethylene Glycol-Coated Copper Nanoparticles and Their Optical Properties

Deborah Okyere [1,2], Ryan H. Manso [1], Xiao Tong [3] and Jingyi Chen [1,2,*]

[1] Department of Chemistry and Biochemistry, University of Arkansas, Fayetteville, AR 72701, USA
[2] Materials Science and Engineering Graduate Program, University of Arkansas, Fayetteville, AR 72701, USA
[3] Center for Functional Nanomaterials, Brookhaven National Laboratory, Upton, NY 11973, USA
* Correspondence: chenj@uark.edu

Abstract: Oxidation is a corrosion reaction where the corroded metal forms an oxide. Prevention of the oxidation at the nanoscale is critically important to retain the physicochemical properties of metal nanoparticles. In this work, we studied the stability of polyethylene glycol (PEG) coated copper nanoparticles (PEGylated CuNPs) against oxidation. The freshly-prepared PEGylated CuNPs mainly consist of metallic Cu which are quite stable in air although their surface is typically covered with a few monolayers of cuprous oxide. However, they are quickly oxidized in water due to the presence of protons that facilitated oxidation of the cuprous oxide to cupric oxide. PEG with carboxylic acid terminus could slightly delay the oxidation process compared to that with thiol terminus. It was found that a solvent with reducing power such as ethanol could greatly enhance the stability of PEGylated CuNPs by preventing the further oxidation of cuprous oxide to cupric oxide and thus retain the optical properties of CuNPs. The reducing environment also assists the galvanic replacement of these PEGylated CuNPs to form hollow nanoshells; however, they consist of ultrasmall particle assemblies due to the co-reduction of gold precursor during replacement reaction. As a result, these nanoshells do not exhibit strong optical property in the near infrared region. This study highlights the importance of solvent effects on PEGylated nonprecious metal nanoparticles against oxidation corrosion and its applications in preserving physicochemical properties of metallic nanostructures.

Keywords: nonprecious metals; oxidation; corrosion; localized surface plasmon resonance; galvanic replacement

Citation: Okyere, D.; Manso, R.H.; Tong, X.; Chen, J. Stability of Polyethylene Glycol-Coated Copper Nanoparticles and Their Optical Properties. *Coatings* **2022**, *12*, x. https://doi.org/10.3390/xxxxx

Academic Editor(s):

Received: date
Accepted: date
Published: date

1. Introduction

Nonprecious metal nanoparticles such as copper nanoparticles (CuNPs) has attracted considerable attentions because of their earth abundance and excellent catalytic activities for diverse chemical reactions [1]. Copper is one of the few metals that exhibits unique optical properties by strongly absorbing and scattering light in the visible to near infrared region [2–5]. Aside from their catalytic and optical properties, Cu nanostructures can find use in printed electronics [6,7] and flexible conductive films [8,9] due to excellent electrical conductivity. These applications rely on the CuNPs remaining in the metallic state; however, CuNPs are prone to be oxidized in air as their surface to volume ratios increase compared to their bulk counterparts. Studies were conducted on the oxidation process and mechanism for the unprotected CuNPs. Yanase et al. found that the oxidation of small CuNPs (5–10 nm) involves a fast reaction of Cu to Cu_2O and a slow reaction of Cu_2O to CuO [10]. While in general the oxidation of CuNPs undergoes Cu → Cu(I) → Cu(II), the kinetics of the process varies by the size of CuNPs and the condition such as temperature and oxygen partial pressure (p). The oxidation of 15 nm CuNPs proceeded significantly slower than that of 4 nm CuNPs at 573 K and p = 0.1 Pa; however, a reverse order was observed at room temperature and p = 10 Pa by van Wijk et al. [11]. The latter

observation is contradictory to the finding by Diociaiuti et al. [12]. that larger particles (30 nm) exhibited slow oxidation in air. This contradiction could perhaps be explained in a study of a self-limiting oxidation process that is directly related to the stress condition in the oxide shell [13]. Moreover, Diaz-Droguett et al. reported that upon exposure to air non-protected CuNPs (10–50 nm) grown under hydrogen using the inert gas condensation method [14] had a Cu(I) shell Cu_2O stabilized by a Cu(II) overlayer CuO [15]. A thermal study by Yabuki et al. indicated a threshold temperature (i.e., 200 °C) for the switch from slow to faster kinetics of Cu(I) to Cu(II) oxide [16].

Despite the considerable interest in the oxidation of Cu nanoparticles on their dry state, it is more intriguing to study their oxidation in solutions due to their use in printed electronics [6,7] and flexible conductive films [8,9]. Corrosion of 50 nm CuNPs and 5 μm Cu microparticles with bare surfaces was studied in water by comparing their oxidation rate [17]. The oxidation rate of nanoparticles sharply increased initially and then level off while the oxidation rate of microparticles slowly increased until ions dissolved in solution reached equilibrium. On the other hand, for liquid phase synthesis, the resulting CuNPs are often protected by surface ligands which prevent the nanoparticles from oxidation to some degree. A number of studies have been conducted to investigate the role of ligands in the oxidation of CuNPs. For example, among a wide range of ligands studied including alkanethiols, phosphines, aliphatic amines, fatty acids, ~3 nm CuNPs capped by alkanethiols or oleic acid in toluene were able to survive from oxidation for a few minutes in air reported by Kanninen et al. [18] which agreed with the results from the previous study of the alkanethioate-protected 1–2 nm CuNPs by Chen et al. [19]. These studies, however, focused on ultra-small particles, the understanding of the ligand effects on large particles is lacking.

On the other hand, different methods have been developed to slow down the oxidation of Cu. For example, CuNPs could be stabilized using a water soluble aminoclay matrix due to its remarkable permselective behavior by blocking the neutral molecule oxygen in contact with CuNPs [20]. Excess oleic acid slightly slowed down the oxidation of these nanoparticles from a few minutes to 30 min while excess of alkanethiols etched away the small CuNPs [18]. Different carboxylic acids were used to prevent oxidation in which lactic acid was the best due to the formation of Cu lactate on the surface [21], and formic acid enabled a copper formate shell to prevent CuNPs from oxidation [22]. Similarly, a thiolate capping ligand with a short alkyl chain and a carboxylic acid end group was found to be the most effective at curbing oxidation in air among eight thiolate capping ligands studied [23]. CuNPs synthesized in presence of poly(allylamine) and allylamine/glycerol were found stable for a long period of time possibly due to the amine group in these agents [24]. Organic corrosion inhibitors such as benzotriazole were used to passivate Cu nanowires and prevent them from oxidation in optoelectronic devices [25]. Other strategies introduced coatings on CuNPs' surfaces to protect CuNPs against oxidation such as a few layers of h-BN or graphene [26-28], carbon [29], barium borosilicate glass [30], polymethyl methacrylate [31], and silver [32,33]. More recently, bare CuNPs grew on the surface of $[Gd_2C]^{2+}\cdot 2e^-$ electride with extremely low work function could be stabilized in air by the excess electrons [34]. Despite these efforts, it remains challenging if or how to stabilize CuNPs in aqueous solution against oxidation.

In this work, we studied the stability of polyethylene glycol (PEG) coated CuNPs (PEGylated CuNPs) suspended in aqueous solution and polar solvents, as well as its influence in the optical properties of CuNPs and the use of PEGylated CuNPs as sacrificed templates in galvanic replacement. PEG is a commonly-used surface capping ligand due to its good solubility in polar solvents and good electrical conductivity that facilitate CuNPs in catalytic and electronic applications [1,7], as well as its biocompatibility making it environmentally friendly [35]. The CuNPs were synthesized by our previously established method in oil phase [5], followed by ligand exchange to replace surface coated organic ligands with PEGs – also referred to as PEGylation process [36,37]. PEGs terminated

with two different functional groups (i.e., PEG-COOH and PEG-SH) were studied respectively. The freshly-prepared PEGylated CuNPs with size of ~50 nm were characterized mainly consisting of metallic Cu and are quite stable in air as dry powders. However, they quickly deteriorated in water due to the proton-associated oxidation and lost their localized surface plasmon resonance (LSPR) properties. A solvent with reducing power such as ethanol can prevent the increase of Cu vacancy and the loss of electron from the surface of the CuNPs and thus greatly enhance the stability of PEGylated CuNPs. Different techniques were employed to characterize nanoparticle morphology, crystal phases, and surface oxidation states of PEGylated CuNPs suspended in water and EtOH to elucidate the oxidation thermodynamics and kinetics. We then examined the use of the PEGylated CuNPs to react with gold salt precursor in the galvanic replacement. It was found that a mild reducing environment could facilitate the formation of hollow nanoshells.

2. Experimental Methods

2.1. Chemicals and Materials

Copper (II) 2,4-pentanedionate ($Cu(acac)_2$, 98%), 1-octadecene (ODE, 90%), tri-n-octylphosphine (TOP, 90%), and tetrachloroauric acid trihydrate ($HAuCl_4 \cdot 3H_2O$) were purchased from Alfa Aesar (Ward Hill, MA). Formic acid (99%), chloroform, and toluene were purchased from EMD (Burlington, MA). Sulfuric acid (ACS grade, 98%) was purchased from BDH (Poole, United Kingdom). Ethanol (100%) was purchased from Coptic (King of Prussia, PA). Oleylamine (OLAM, 70%), methoxypolyethylene glycol thiol (PEG-SH, M.W.= 5000), and methoxypolyethylene glycol acetic acid (PEG-COOH, M.W.= 5000) were purchased from Sigma Aldrich (St. Louis, MO). Isopropyl Alcohol (isopropanol) was purchased from Macron Chemicals (Radnor, PA). All experiments were conducted using 18 MΩ H_2O unless otherwise stated. All chemicals were used as received.

2.2. Synthesis of PEGyated CuNPs

The CuNPs were synthesized using our previously established method in oil phase [5]. Briefly, 52.4 mg of $Cu(acac)_2$ was added into a 25 mL three-neck round-bottom flask containing 4 mL of ODE and 1 mL of OLAM under the protection of N_2. After the addition of 1 mL of TOP, the reaction mixture was heated under N_2 protection. When the temperature reached to 200 °C, small amount of CO produced by reacting 10 mL each of formic acid and sulfuric acid was introduced into the reaction mixture for 10 s. After the temperature reached 220 °C, the reaction mixture turned a deep red color, indicating the formation of CuNPs. The reaction was then allowed to run for an additional 20 min before it was quenched by removing the heating mantle and allowed to cool to room temperature. The product was transferred into a 50 mL centrifuge tube, followed by adding a mixture of ethanol and toluene (4:1). The CuNPs were collected by centrifuging at 8000 rpm for 5 min and redispersed in 3 mL of toluene.

For ligand transfer, 3 mL of the as-prepared CuNPs were added to 10 mL chloroform containing 1 mg/mL PEG-SH or PEG-COOH. The mixture was stirred at room temperature for 8 h. The suspension was evenly distributed into two centrifuge tubes filled each with 30 mL of hexane. The PEGylated CuNPs (either PEG-SH coated CuNPs or PEG-COOH coated CuNPs) were collected by centrifuging at 10,000 rpm for 10 min. The resulting pellets were dispersed in ethanol, transferred in 1.5 mL centrifuged tubes, and centrifuged at 14,000 rpm for 30 min. After removing the supernatant, the pellets were dispersed in water and purified twice at 14,000 rpm for 20 min at 4 °C. The resulting PEGylated CuNPs were dispersed in 4 mL of solvents (i.e., water, ethanol, or isopropanol).

2.3. Galvanic Replacement of PEG-Coated CuNPs with Gold Precursor

A total volume of 200 μL of as-prepared PEG-coated CuNPs was diluted to 2 mL with different solvents (i.e., water, ethanol, or isopropanol) and their absorbance was taken. A concentration of 1 mM $HAuCl_4$ with a total volume of 0.1 mL was added at a rate

of 0.001 mL/s to the above 2 mL PEG-coated CuNPs in a round bottom flask under continuous magnetic stirring. The absorbance after the reaction was measured. The resulting mixture was centrifuged at 14,000 rpm for 30 min, and the pellet was washed twice with the corresponding solvent at 14,000 rpm for 15 min. The final product was dispersed in the corresponding solvent ready for characterization.

2.4. Characterization

Transmission electron microscopy (TEM) images were obtained using a transmission electron microscope (JEOL JEM-1011) with an accelerating voltage of 100kV. Samples were prepared by drop casting 3 μL of particle suspension onto Cu mesh TEM grids and allowed to air dry before imaging. X-ray powder diffraction (XRD) was performed using a benchtop X-ray diffractometer (Rigaku Miniflex II) with operation at 30 kV/15 mA and with Cu Kα radiation as the source. Each sample was prepared by drop casting about 60 μL of sample onto a zero diffraction Si_2O substrate with 10 μL at a time to form an even thickness and subsequently drying each layer with a stream of nitrogen. UV-Vis spectra were obtained using UV-vis spectrophotometer (Agilent Cary 50). XPS experiments were conducted with an ultrahigh vacuum (UHV) which has base pressures < 5 ×10^{-9} Torr and equipped with a hemispherical electron energy analyzer (SPECS, PHOIBOS 100) and twin anode X-ray source (SPECS, XR50). Samples were prepared by drop casting about 50 μL of each sample on clean Si substrates and gently drying with a stream of nitrogen. The radiation source was Al Kα(1486.6 eV) which was used at 15 kV and 20 mA. The analyzer and x-ray source had an angle of 45° between them and photoelectrons were collected along the sample surface normal. CasaXPS software was used to analyze the XPS spectra.

3. Results and Discussion

The CuNPs were synthesized by our previously established protocol by reducing Cu precursor in the presence of OLAM and TOP. These OLAM/TOP coated CuNPs were then reacted with PEG-COOH or PEG-SH in chloroform that allowed the ligand exchange process to take place in a miscible phase, illustrated in Figure 1A. The PEG molecules are able to replace OLAM/TOP on the surface of CuNPs and coordinate to Cu surface similar to the interaction of crown ether-metal ion chelating [38]. Additional PEG molecules could continue coating to CuNPs' surface through van der Waals interaction (i.e. hydrogen bonding) to increase PEG coating thickness depending on the PEGylation time. Figure 1, B-D, displays the TEM images of the CuNPs before and after ligand exchange process for 8 h. The histogram of size distribution analysis on the TEM image of each sample were plotted in Figure S1. The size of the OLAM/TOP coated CuNPs was estimated to be 34.8 ± 5.0 nm. The PEGylated CuNPs slightly increased in their size to 40.8 ± 5.3 nm and 42.3 ± 5.6 nm, for PEG-COOH and PEG-SH, respectively. The size increase is corresponding to the thickness of the PEG coating estimated to be 3–4 nm.

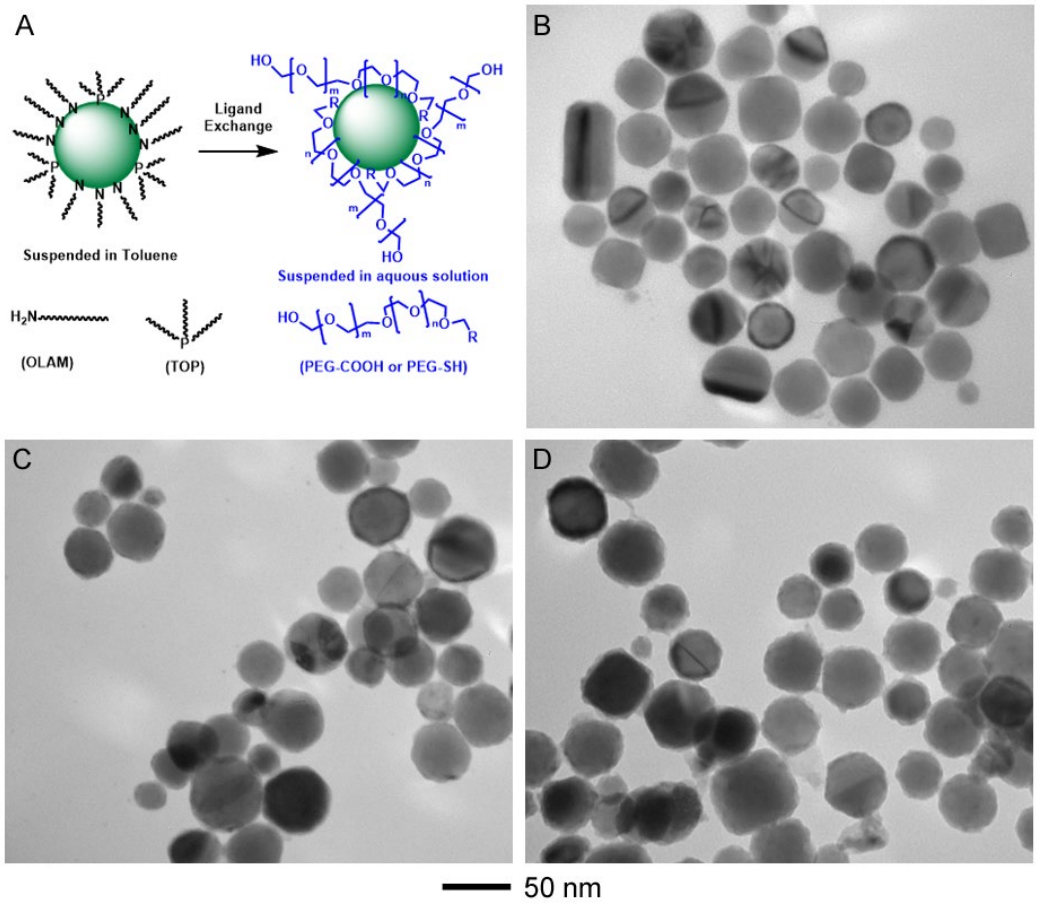

Figure 1. (**A**) Schematic illustration of the ligand exchange reaction where the OLAM/TOP ligands on CuNPs were replaced by PEG-COOH or PEG-SH. (**B–D**) TEM images of OLAM/TOP coated CuNPs (**B**); PEG-COOH coated CuNPs (**C**); and PEG-SH coated CuNPs (D).

After the ligand displacement reaction, the PEGylated CuNPs could be suspended in aqueous solution. We monitored their stability by UV-vis spectroscopy and XRD. It is known that the CuNPs exhibit LSPR in the visible region. The OLAM/TOP CuNPs have an LSPR at ~610 nm in their UV-vis spectrum and XRD shows their crystal structure of face-centered-cubic (fcc) phase (Figure S2). These PEGylated coated CuNPs with a size of ~40 nm diameter displayed an LSPR at 610 nm; however, the LSPR feature quickly became broadening and shifted to the red after the CuNPs were suspended in water for a day (Figure 2, A and B). It is suggested the surface of CuNPs is likely oxidized. The speculation was verified by the chemical composition analysis by XRD where Cu_2O was co-existed with Cu in the XRD patterns of the samples after a few days suspended in water (Figure 2, C and D). The x-ray reflection peaks at 43.3, 50.3, and 74.1 degree were assigned to fcc Cu crystal structure while those at 36.2, 42.2, and 61.3 degree were indexed to cubic cuprous oxide Cu_2O [39]. The oxidation of metallic Cu to cuprous oxide is a spontaneous process at standard condition ($4Cu(s) + O_2(g) \rightarrow 2Cu_2O(s)$; $\Delta_r G^o = -292 kJ / mol$). The PEG-coated CuNPs could be oxidized in air; but it was very slow. They could be kept in dry air for a prolonged period of time with little change in their fcc Cu XRD pattern (Figure S3). However, the oxidation could be accelerated in moist air or in water by displacing Cu in the cuprous oxide by protons and thus lowering the activation energy of oxidation [40]. The further oxidation of Cu_2O to cupric oxide CuO ($2Cu_2O(s) \rightarrow 4CuO(s)$; $\Delta_r G^o = -226.8 kJ / mol$) was observed in these PEGylated CuNPs as indicated by the small reflection peak at 29.5 degree in the XRD patterns of the oxidized samples. The reflection peak can be indexed to the (002) crystallography plane of the monoclinic CuO [26]. Different terminus of the PEG chain has some effect on the oxidation process. PEG-COOH

coated CuNPs has a slight delay in the oxidation as indicated by a slightly lower content of Cu_2O when comparing the relative peak intensity of Cu_2O (111) to Cu (111). This could be attributed to the lower pK_a of carboxylic acid (pK_a = 4-5) than that of thiol (pK_a = 10) that some surface Cu_2O/CuO could be dissolved in PEG-COOH solution. It agreed with other studies that carboxylic acid (i.e. acetic acid) was used to remove surface oxides of Cu nanostructures [4, 41]. Further incubation of PEGylated CuNPs in water increased the degree of oxidation. The relative peak intensity of Cu_2O (111) to Cu (111) increased and the CuO (002) reflection became more obvious in the XRD patterns obtained after 5 days suspended in water for both PEG-COOH and PEG-SH capping ligands (Figure S4).

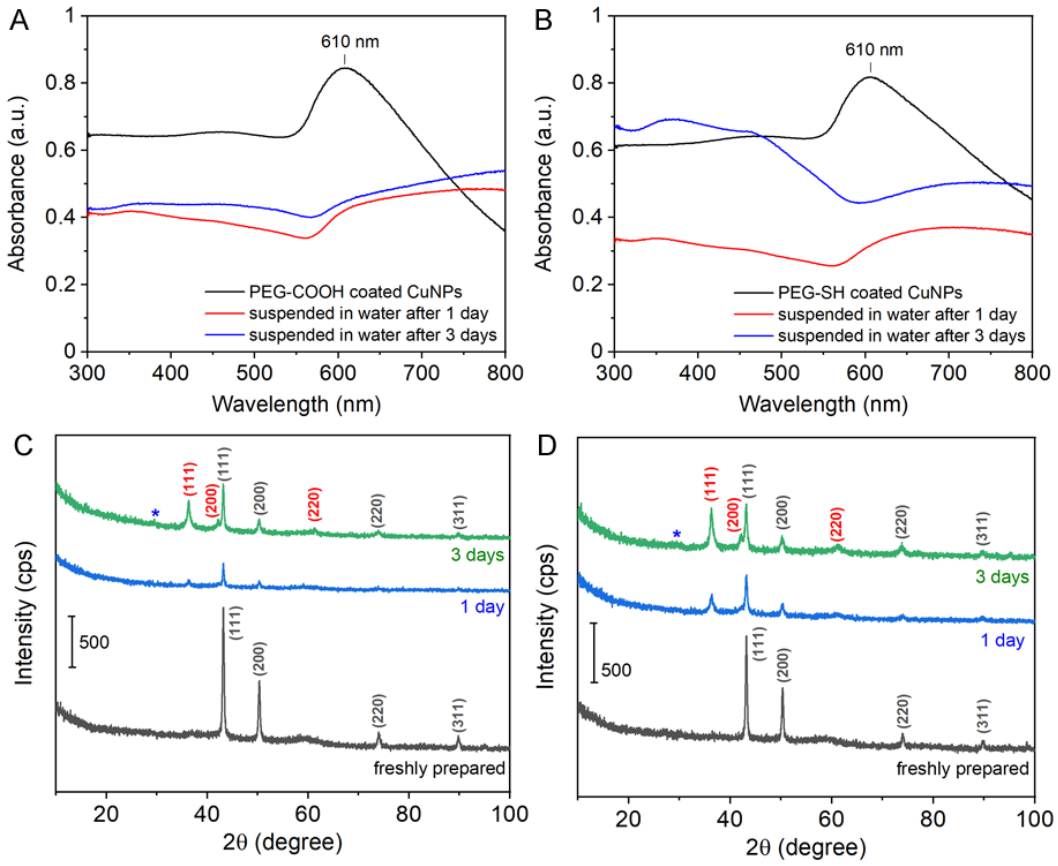

Figure 2. (**A**,**B**) UV-vis spectra of PEGylated CuNPs: (**A**) PEG-COOH; and (**B**) PEG-SH. Spectra in black, red, and blue was taken immediately after, after 1 day, and 3 days suspended in water, respectively. (C,D) XRD of the PEGylated CuNPs: (**C**) PEG-COOH; and (**D**) PEG-SH. The reflection peaks labeled in black and red are corresponding to the indices for fcc Cu and cubic Cu_2O, respectively. The peak labeled with blue star is indexed to (002) of monoclinic CuO.

The oxidation of PEGylated CuNPs was further characterized by TEM and XPS for the samples suspended in water after 5 days. It is known that cuprous oxide is metal deficient ($Cu_{2-\delta}O$) and results in Cu vacancies in Cu sub-lattice [42–45]. The oxidation of Cu takes place by the transport of Cu^{2+} and electrons through Cu vacancies ($V_{Cu}^{'}$, a single charged cation vacancy) and electron holes ($h^{\bullet}$, an electron hole) in cuprous oxide [32,33]. The formation of the vacancies can be described by the reaction in air ($\frac{1}{4}O_2(g) + Cu_{Cu} \rightleftharpoons V_{Cu}^{'} + h^{\bullet} + \frac{1}{2}O_o$) or in the presence of water ($\frac{1}{2}H_2O(g) + Cu_{Cu} \rightleftharpoons V_{Cu}^{'} + h^{\bullet} + \frac{1}{2}O_o$), where Cu_{Cu} and O_o are the neutral cation and anion lattice site, respectively. Compared to dry air, water indeed increased the Cu vacancies and facilitate the electrons of the intermediate Cu_2O thereby accelerating the oxidative corrosion of the CuNPs. As proton in water accelerate the corrosion process, oxidation of PEG-coated CuNPs could be visualized by examining the CuNPs after suspended in water for

5 days under TEM. The oxidation occurred inhomogeneously with some CuNPs corroded much faster than the others. For example, a thick layer of oxides could be seen covering the surface of CuNPs (Figure 3A) while some of the oxides were hollowed out (Figure 3B), indicative of the formation of the Cu vacancies in Cu_2O during the oxidative corrosion. The dissolved Cu^+/Cu^{2+} from the CuNPs could nucleate/deposit to the dissolving CuNPs or self-nucleate, resulted in the formation of particulates with irregular shapes of size ranging from 50 nm to several hundred nanometers.

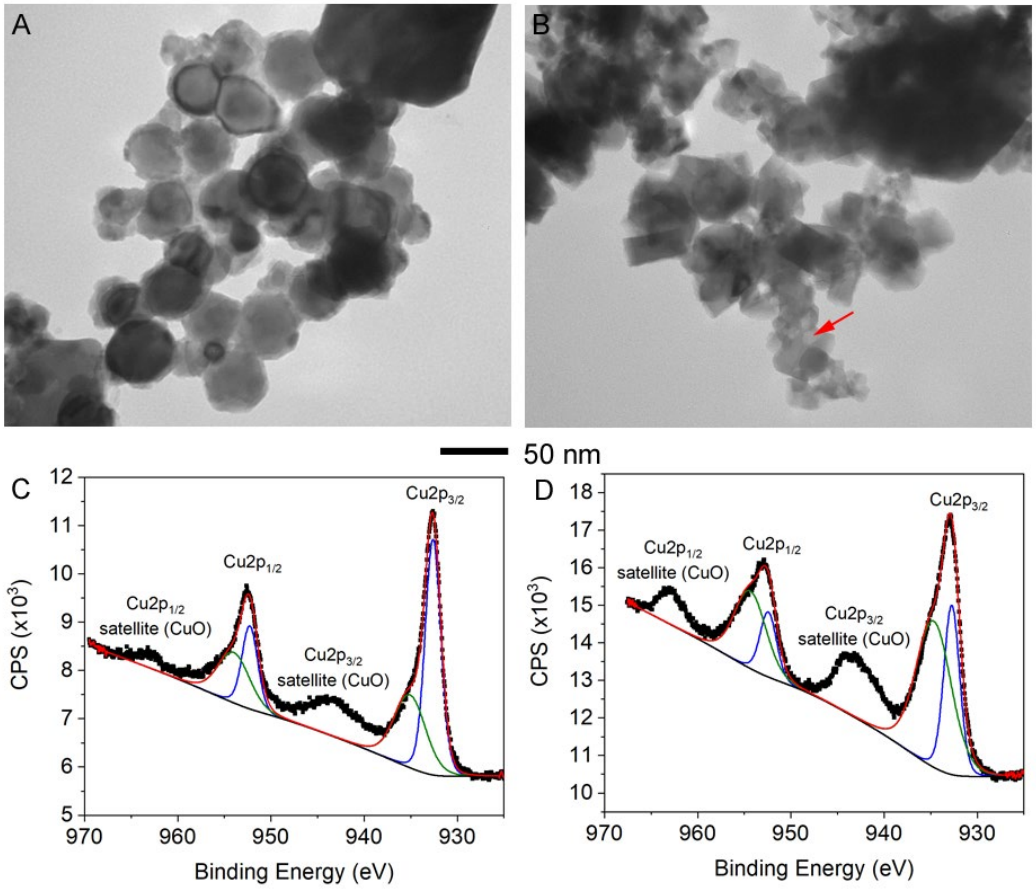

Figure 3. (**A**,**B**) TEM images of PEG-SH coated CuNPs after suspended in water for 5 days indicated inhomogeneous oxidation. The surface of the CuNPs was covered by Cu_2O/CuO with porous feature indicated by a red arrow. (**C**,**D**) Cu2p XPS of the PEG-SH coated CuNPs freshly prepared (**C**) and after 5 days suspended in water (**D**). The red curve is the sum of blue and green curves that fit $Cu2p_{3/2}$ and $Cu2p_{1/2}$ regions with Cu/Cu_2O and CuO, respectively.

The samples were further analyzed by XPS to investigate the surface oxidation of the CuNP film within 10 nm from the top surface. Figure C and D display the Cu2p XPS of the samples before and after 5 days suspended in water. The relative intensity of satellite broad bands of CuO at 940–950 eV ($Cu2p_{3/2}$) and 960–970 eV ($Cu2p_{1/2}$) [48] increased after suspended in water for 5 days. The quantitative analysis of $Cu2p_{3/2}$ and $Cu2p_{1/2}$ peak fittings indicated that the CuO component increased from 46.1% to 67.6% after suspended in water for 5 days. Assuming that the thin film consisted of a monolayer of 50 nm CuNPs, roughly 20 at.% of a CuNP could be probed by XPS with a 10 nm penetration depth. For the CuNPs, the CuO content increased from less than half of 10 at.% to above 10 at.% crossing the detection limit of the XRD (~10%), agreed well with the XRD result.

Can we introduce an environment suited for improving the stability of PEG-coated CuNPs in the suspension? One can hypothesize that a solvent can reduce the Cu vacancies and prevent loss of electrons in order to improve their stability. We test this hypothesis by suspending the PEG-SH coated CuNPs in alcohol such as ethanol which is frequently

used as a reducing agent in colloidal synthesis. Compared to water, we observed great improvement for the stability PEG-coated CuNPs in ethanol. The LSPR peak of the CuNPs at 610 nm remained unchanged in their optical spectra after 3 weeks suspended in ethanol (Figure 4A). For comparison with those suspended in water, we characterized the PEG-coated CuNPs suspended in ethanol for 5 days by XRD and XPS. The XRD pattern remained oxide free after 5 days suspended in ethanol where the peaks at 43.3, 50.3, 74.1, and 89.7 degree were assigned to fcc Cu, as shown in Figure 4B. The surface oxidation of these CuNPs was characterized by XPS (Figure 4 C,D). The relative intensity of CuO satellite broad band slightly increased. The XPS indicated that the surface CuO on the CuNPs increased 35.6% to 49.4%; however, it remained below the detection limit of XRD. Similar trend was observed in the XPS spectra for the PEG-COOH coated CuNPs where ethanol prevented further oxidation of the surface Cu (Figure S5).

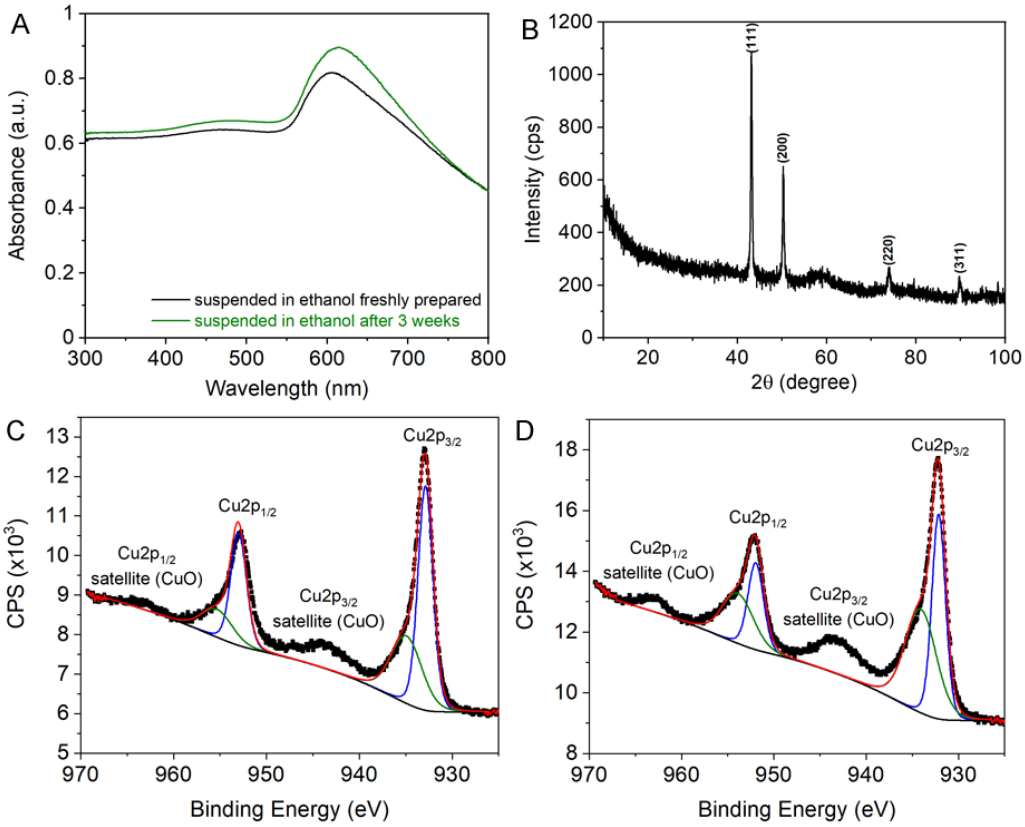

Figure 4. (**A**) UV-vis spectra of the PEG-SH coated CuNPs suspended in ethanol freshly prepared and after 3 weeks. (**B**) XRD of the PEG-SH coated CuNPs after 5 day suspended in ethanol. (**C**,**D**) Cu2p XPS of the PEG-SH coated CuNPs freshly prepared (**C**) and after 5 days suspended in ethanol (**D**). The red curve is the sum of blue and green curves that fit $Cu2p_{3/2}$ and $Cu2p_{1/2}$ regions with Cu/Cu_2O and CuO, respectively.

Since it is difficult to differentiate Cu(I) from Cu(0) from $Cu2p_{3/2}$, Cu LMM peak shape can be useful in determining Cu chemical states [48,49]. Figure 5 displays Cu LMM spectra (black curves) corresponding to the samples in Figure 3, C and D, as well Figure 4, C and D. By comparing the Cu LMM peak shape, the PEG-SH coated CuNPs suspended in ethanol were less oxidized than those suspended in water immediately after preparation, as shown in Figure 5, A and C, respectively. After 5 days, the suspension in aqueous solution became more oxidized (Figure 5B) while the suspension in ethanol appeared to be reduced (Figure 5D). For all these samples, 10 min of Ar sputtering completely removed the oxide exposed on their surfaces as indicated in the blue curves of each panel in Figure 5 which was corresponding to a few monolayers of atoms. This observation was confirmed by the Cu2p XPS spectra where the satellite peaks disappeared (Figure S6). The

Cu LMM-Cu2p$_{3/2}$ peak position for each sample was analyzed and compared to literature (Figure S7) [49]. The result agreed well with the Cu LMM peak shape analysis. The surface of freshly prepared PEG-coated CuNPs was covered by a mixture of Cu_2O (916.8 eV) and CuO/Cu at (917.7/918.6 eV). CuNPs in ethanol is more metallic as indicated by the shoulder peak at ~921 eV. Water facilitated the oxidation of Cu → Cu_2O → CuO, and therefore after 5 days in water, the surface is dominated by Cu_2O along with more CuO. In ethanol, the surface was covered by CuO/Cu possibly because Cu_2O was reduced to Cu by ethanol. From these results along with the XRD and TEM analysis, the alcohol solvent indeed provided a reducing environment to improve the stability of PEG-coated CuNPs.

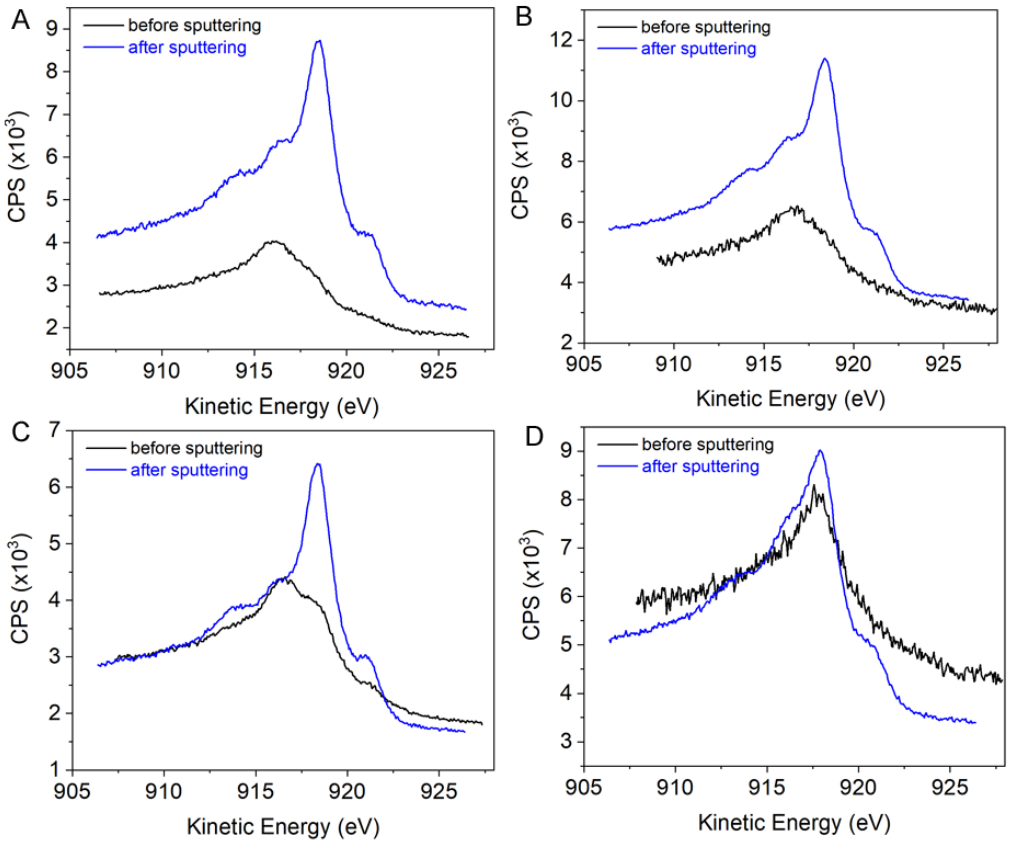

Figure 5. Cu LMM spectra of the PEG-SH coated CuNPs: (**A**) suspended in water freshly prepared; (**B**) suspended in water for 5 days; (**C**) suspended in ethanol freshly prepared; (**D**) suspended in ethanol after 5 days. The black curves are the spectra of the pristine samples while the blue curves are the corresponding samples treated with 10 min of Ar sputtering to remove a few monolayers of atoms from the surface.

We further explored how the stability of PEGylated CuNPs affects their use as sacrificed templates in the galvanic replacement reaction. The galvanic replacement at the nanoscale has been documented in the literature between Ag nanostructures and the Au salt precursor ($HAuCl_4$) [50,51]. However, to replace Ag with nonprecious metals such as Cu, it encounters the challenges due to their instability and fast replacement kinetics in aqueous solution. Figure 6A displays the TEM image of the product of the galvanic replacement between the PEG-SH coated CuNPs and $HAuCl_4$ in water. Due to the instantaneous oxidation of these CuNPs by $HAuCl_4$ in aqueous solution, the galvanic replacement yielded a mixture of collapsed hollow shells consisting of small Au clusters and agglomerates of Au clusters. As a result, the LSPR blue shifted to 590 nm after the reaction, as shown in Figure 6, B and C. We then performed the galvanic replacement in ethanol where the PEG-SH coated CuNPs dispersed in ethanol was reacted with $HAuCl_4$. Due to the strong reducing power of ethanol, the gold precursor Au(III) was quickly reduced to

Au(0) that either deposits on the CuNPs or self-nucleates to form Au nanoparticles (Figure 6D). The LSPR also blue shifted after the reaction (Figure 6, E and F). To slow down the reduction of Au but still maintain a reducing environment, ethanol was switched to isopropanol. The TEM image indicated that hollow nanoshells were formed, as shown in Figure 6G; however, the nanoshells were composed of ultra-small Au clusters instead of smooth shells. As a result, the corresponding LSPR blue shifted similar to that of the product in ethanol (Figure 6, H and I). In all cases, the LSPR appeared to be suppressed possible due to the existing of oxides mixed/adjacent to Au clusters similar to the finding by others [52]. Similar trend was found for the galvanic replacement of PEG-COOH coated CuNPs, suggesting that the terminus has little effect in the reaction. Although further optimization of the reaction is needed to slow down the reduction kinetics of Au, the result warrants the future investigation of galvanic replacement in a reducing environment for CuNPs to form hollow Au shells.

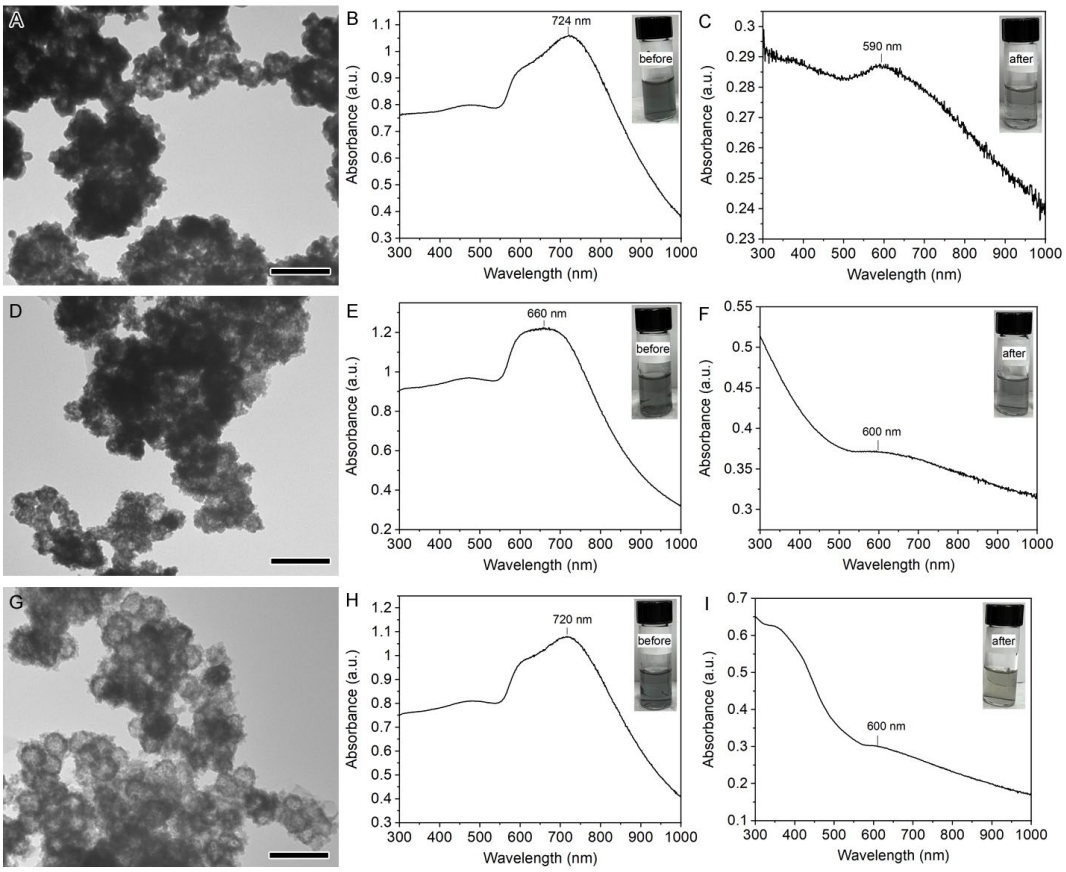

Figure 6. TEM images of products and UV-vis spectra before and after the galvanic replacement reaction between PEG-SH coated CuNPs and $HAuCl_4$ in different solvents: (**A-C**) water; (**D-F**) ethanol; and (**G-I**) isopropanol. The scale bar is 100 nm.

4. Conclusion

We prepared PEGylated CuNPs with either PEG-SH or PEG-COOH through the ligand exchange process of the OLAM/TOP coated CuNPs in chloroform. The freshly prepared PEGylated CuNPs were characterized by XRD as metallic fcc Cu, but their surfaces were covered by a few monolayers of Cu_2O and CuO. Solvent plays a critical role on the stability of these PEGylated CuNPs. In aqueous solution, these PEGylated CuNPs quickly lost their optical properties due to the proton-facilitated oxidation. Carboxylic acid terminated PEG could slightly delay the oxidation compared to thiol terminated PEG. However, the oxidation corrosion could be prevented by suspending in a solvent with reducing power such as alcohol. XPS reveals that ethanol can inhibit Cu_2O from further oxidation

to CuO and thus enhance the stability of the PEGylated CuNPs and retain their optical properties. Furthermore, by controlling the reducing environment, these PEGylated CuNPs could serve as sacrificed templates in the galvanic replacement to form hollow Au nanoshells. However, further balancing the kinetics of the galvanic replacement of CuNPs and the reduction of Au is needed to yield nanoshells with continuous walls that exhibits near-infrared optical properties. This study provides insights of the solvent effects on PEGylated nonprecious metal nanoparticles against oxidation corrosion and its applications in preserving physicochemical properties of metallic nanostructures.

Supplementary Materials: Page: 11
The following supporting information can be downloaded at: www.mdpi.com/xxx/s1, Figure S1: Histograms of size distribution analysis of different CuNPs on the TEMs in Figure 1, B-D: (A) CuNPs; (B) PEG-COOH coated CuNPs; and (C) PEG-SH coated CuNPs.; Figure S2: Characterization of OLAM/TOP CuNPs suspended in toluene: (A) UV-vis spectrum showing LSPR at 610 nm; and (B) XRD pattern indicating face-centered-cubic (fcc) Cu.; Figure S3: (A) XRD pattern of the PEG-SH coated CuNPs kept in air for 5 days showing no change of the fcc metallic Cu phase. (B) XRD pattern of the SiO_2 substrate, indicated that the weak broad band around 60 degree in (A) is from the SiO_2 substrate.; Figure S4: XRD patterns of PEGylated CuNPs suspended in water after 5 days: (A) PEG-COOH coated CuNPs; and (B) PEG-SH coated CuNPs. The reflection peaks labeled in black and red are corresponding to the indices for fcc Cu and cubic Cu_2O, respectively. The peak labeled with blue star is indexed to (002) of monoclinic CuO.; Figure S5: Cu2p XPS and LMM spectra of the PEG-COOH coated CuNPs samples suspended in different solvents for 5 days: (A,B) water; and (C,D) ethanol.; Figure S6: Cu2p XPS of the corresponding PEG-SH coated CuNPs samples in Figure 3, C and D, as well as Figure 4, C and D after 10 min of Ar sputtering to remove surface oxides: (A) sample suspended in water freshly prepared; (B) sample suspended in water for 5 days; (C) sample suspended in ethanol freshly prepared; and (D) sample suspended in ethanol for 5 days.; Figure S7: (Top) The plot of Cu LMM peak position versus $Cu2p_{3/2}$ peak position for samples before sputtering (black square) and after sputtering (red square). The labels, A to D, are corresponding to: (A) sample suspended in water freshly prepared; (B) sample suspended in water for 5 days; (C) sample suspended in ethanol freshly prepared; and (D) sample suspended in ethanol for 5 days. (Bottom) The plot of Cu LMM peak position versus $Cu2p_{3/2}$ peak position for different substance from the literature (*Surface and Interface Analysis*, 2017, *49*, 1325).; Figure S8: TEM images of products and UV-vis spectra before and after the galvanic replacement reaction between PEG-COOH coated CuNPs and $HAuCl_4$ in different solvents: (A-C) water; (D-F) ethanol; and (G-I) isopropanol. The scale bar is 100 nm.

Funding: This work was supported by the grant from National Science Foundation NSF CBET 1826642. XPS measurements were performed at the Center for Functional Nanomaterials (CFN), which is a U.S. DOE Office of Science Facility, at BNL under Contract No. DE-SC0012704.

Author Contributions: Conceptualization, J.C.; Methodology, D.O., R.M., X.T., and J.C.; Investigation, D.O., R.M., X.T.; Data Curation, D.O. and J.C.; Writing – Original Draft Preparation, J.C.; Writing – Review & Editing, D.O., R.M.; X.T. and J.C.

Data Availability: Data is contained within the article or supplementary material.

Conflicts of Interest: The authors declare no conflict of interest.

References

1. Gawande, M.B.; Goswami, A.; Felpin, F.-X.; Asefa, T.; Huang, X.; Silva, R.; Zou, X.; Zboril, R.; Varma, R.S., Cu and Cu-Based Nanoparticles: Synthesis and Applications in Catalysis. *Chem. Rev.* **2016**, *116*, 3722-3811.
2. Kim, S.; Kim, J.-M.; Park, J.-E.; Nam, J.-M., Nonnoble-Metal-Based Plasmonic Nanomaterials: Recent Advances and Future Perspectives. *Adv. Mater.* **2018**, *30*, 1704528.
3. Wang, H.; Tam, F.; Grady, N.K.; Halas, N.J., Cu Nanoshells: Effects of Interband Transitions on the Nanoparticle Plasmon Resonance. *J. Phys. Chem. B* **2005**, *109*, 18218-18222.
4. Chan, G.H.; Zhao, J.; Hicks, E.M.; Schatz, G.C.; Van Duyne, R.P., Plasmonic Properties of Copper Nanoparticles Fabricated by Nanosphere Lithography. *Nano Lett.* **2007**, *7*, 1947-1952.

5. Crane, C.C.; Wang, F.; Li, J.; Tao, J.; Zhu, Y.; Chen, J., Synthesis of Copper–Silica Core–Shell Nanostructures with Sharp and Stable Localized Surface Plasmon Resonance. *J. Phys. Chem. C* **2017**, *121*, 5684-5692.
6. Lee, Y.; Choi, J.-r.; Lee, K.J.; Stott, N.E.; Kim, D., Large-Scale Synthesis of Copper Nanoparticles by Chemically Controlled Reduction for Applications of Inkjet-Printed Electronics. *Nanotechnology* **2008**, *19*, 415604.
7. Magdassi, S.; Grouchko, M.; Kamyshny, A., Copper Nanoparticles for Printed Electronics: Routes Towards Achieving Oxidation Stability. *Materials* **2010**, *3*, 4626-4638.
8. Rathmell, A.R.; Bergin, S.M.; Hua, Y.-L.; Li, Z.-Y.; Wiley, B.J., The Growth Mechanism of Copper Nanowires and Their Properties in Flexible, Transparent Conducting Films. *Adv. Mater.* **2010**, *22*, 3558-3563.
9. Yang, H.-J.; He, S.-Y.; Chen, H.-L.; Tuan, H.-Y., Monodisperse Copper Nanocubes: Synthesis, Self-Assembly, and Large-Area Dense-Packed Films. *Chem. Mater.* **2014**, *26*, 1785-1793.
10. Yanase, A.; Komiyama, H., In Situ Observation of Oxidation and Reduction of Small Supported Copper Particles Using Optical Absorption and X-Ray Diffraction. *Surf. Sci.* **1991**, *248*, 11-19.
11. van Wijk, R.; Görts, P.C.; Mens, A.J.M.; Gijzeman, O.L.J.; Habraken, F.H.P.M.; Geus, J.W., XPS/NRA Investigations of Particle Size Effects During the Oxidation of Cu Particles Supported on Oxidised Si (100). *Appl. Surf. Sci.* **1995**, *90*, 261-269.
12. Diociaiuti, M.; Bascelli, A.; Paoletti, L., Extended Energy Loss Fine Structure and Selected Area Electron Diffraction Combined Study of Copper Cluster Oxidation. *Vacuum* **1992**, *43*, 575-581.
13. Chen, C.-H.; Yamaguchi, T.; Sugawara, K.-i.; Koga, K., Role of Stress in the Self-Limiting Oxidation of Copper Nanoparticles. *J. Phys. Chem. B* **2005**, *109*, 20669-20672.
14. Granqvist, C.G.; Buhrman, R.A., Ultrafine Metal Particles. *J. Appl. Phys.* **1976**, *47*, 2200-2219.
15. Diaz-Droguett, D.E.; Espinoza, R.; Fuenzalida, V., Copper Nanoparticles Grown under Hydrogen: Study of the Surface Oxide. *Appl. Surf. Sci.* **2011**, *257*, 4597-4602.
16. Yabuki, A.; Tanaka, S., Oxidation Behavior of Copper Nanoparticles at Low Temperature. *Mater. Res. Bull.* **2011**, *46*, 2323-2327.
17. Xia, X.; Xie, C.; Cai, S.; Yang, Z.; Yang, X., Corrosion Characteristics of Copper Microparticles and Copper Nanoparticles in Distilled Water. *Corros. Sci.* **2006**, *48*, 3924-3932.
18. Kanninen, P.; Johans, C.; Merta, J.; Kontturi, K., Influence of Ligand Structure on the Stability and Oxidation of Copper Nanoparticles. *J. Colloid Interface Sci.* **2008**, *318*, 88-95.
19. Chen, S.; Sommers, J.M., Alkanethiolate-Protected Copper Nanoparticles: Spectroscopy, Electrochemistry, and Solid-State Morphological Evolution. *J. Phys. Chem. B* **2001**, *105*, 8816-8820.
20. Datta, K.; Kulkarni, C.; Eswaramoorthy, M., Aminoclay: A Permselective Matrix to Stabilize Copper Nanoparticles. *Chem. Commun.* **2010**, *46*, 616-618.
21. Deng, D.; Cheng, Y.; Jin, Y.; Qi, T.; Xiao, F., Antioxidative Effect of Lactic Acid-Stabilized Copper Nanoparticles Prepared in Aqueous Solution. *J. Mater. Chem.* **2012**, *22*, 23989-23995.
22. Kim, I.; Kim, Y.; Woo, K.; Ryu, E.-H.; Yon, K.-Y.; Cao, G.; Moon, J., Synthesis of Oxidation-Resistant Core–Shell Copper Nanoparticles. *RSC Adv.* **2013**, *3*, 15169-15177.
23. Dabera, G. D. M. R.; Walker, M.; Sanchez, A. M.; Pereira, H. J.; Beanland, R.; Hatton, R. A., Retarding Oxidation of Copper Nanoparticles without Electrical Isolation and the Size Dependence of Work Function. *Nature Commun.* **2017**, *8*, 1894.
24. Jardón-Maximino, N.; Pérez-Alvarez, M.; Sierra-Ávila, R.; Ávila-Orta, C. A.; Jiménez-Regalado, E.; Bello, A. M.; González-Morones, P.; Cadenas-Pliego, G., Oxidation of Copper Nanoparticles Protected with Different Coatings and Stored under Ambient Conditions. *J. Nanomater.* **2018**, *2018*, 9512768.
25. Polat Genlik, S.; Tigan, D.; Kocak, Y.; Ercan, K. E.; Cicek, M. O.; Tunca, S.; Koylan, S.; Coskun, S.; Ozensoy, E.; Unalan, H. E., All-Solution-Processed, Oxidation-Resistant Copper Nanowire Networks for Optoelectronic Applications with Year-Long Stability. *ACS Appl. Mater. Interfaces* **2020**, *12*, 45136-45144.
26. Fan, D.; Zhou, Q.; Lv, X.; Jing, J.; Ye, Z.; Shao, S.; Xie, J., Synthesis, Thermal Conductivity and Anti-Oxidation Properties of Copper Nanoparticles Encapsulated within Few-Layer H-Bn. *Ceramics Inter.* **2018**, *44*, 1205-1208.
27. Zhang, Y.; Li, N.; Xiang, Y.; Wang, D.; Zhang, P.; Wang, Y.; Lu, S.; Xu, R.; Zhao, J., A Flexible Non-Enzymatic Glucose Sensor Based on Copper Nanoparticles Anchored on Laser-Induced Graphene. *Carbon* **2020**, *156*, 506-513.
28. Scardamaglia, M.; Boix, V.; D'Acunto, G.; Struzzi, C.; Reckinger, N.; Chen, X.; Shivayogimath, A.; Booth, T.; Knudsen, J., Comparative Study of Copper Oxidation Protection with Graphene and Hexagonal Boron Nitride. *Carbon* **2021**, *171*, 610-617.
29. Zhou, X.; Guo, W.; Zhu, Y.; Peng, P., The Laser Writing of Highly Conductive and Anti-Oxidative Copper Structures in Liquid. *Nanoscale* **2020**, *12*, 563-571.
30. Jung, D. S.; Koo, H. Y.; Wang, S. E.; Park, S. B.; Kang, Y. C., Ultrasonic Spray Pyrolysis for Air-Stable Copper Particles and Their Conductive Films. *Acta Mater.* **2021**, *206*, 116569.
31. Yu, S.; Li, J.; Zhao, L.; Gong, B.; Li, L., Folding-Insensitive, Flexible Transparent Conductive Electrodes Based on Copper Nanowires. *Sol. Energy Mater. .Sol. Cells* **2021**, *231*, 111323.
32. Varol, T.; Hacısalihoğlu, İ.; Kaya, G.; Güler, O.; Yıldız, F.; Aksa, H. C.; Akçay, S. B., The Effect of Selective Laser Melting Process on the Microstructure, Density, and Electrical Conductivity of Silver-Coated Copper Cores. *Journal of Materials Engineering and Performance* **2021**, *30*, 5216-5226.

33. Zareei, A.; Gopalakrishnan, S.; Mutlu, Z.; He, Z.; Peana, S.; Wang, H.; Rahimi, R., Highly Conductive Copper–Silver Bimodal Paste for Low-Cost Printed Electronics. *ACS Appl. Electron. Mater.* **2021**, *3*, 3352-3364.
34. Chung, K.; Bang, J.; Thacharon, A.; Song, H. Y.; Kang, S. H.; Jang, W.-S.; Dhull, N.; Thapa, D.; Ajmal, C. M.; Song, B., Non-Oxidized Bare Copper Nanoparticles with Surface Excess Electrons in Air. *Nature Nanotech.* **2022**, *17*, 285-291.
35. Zalipsky, S.; Harris, J. M., Introduction to Chemistry and Biological Applications of Poly(Ethylene Glycol). In *Poly(Ethylene Glycol)*, American Chemical Society: 1997; Vol. 680, pp 1-13.
36. Chen, S.; Jenkins, S.V.; Tao, J.; Zhu, Y.; Chen, J., Anisotropic Seeded Growth of Cu–M (M = Au, Pt, or Pd) Bimetallic Nanorods with Tunable Optical and Catalytic Properties. *J. Phys. Chem. C* **2013**, *117*, 8924-8932.
37. Jenkins, S.V.; Chen, S.; Chen, J., Gold–Copper Alloyed Nanorods for Metal-Catalyzed Organic Reactions: Implication of Surface Ligands on Nanoparticle-Based Heterogeneous Catalysis. *Tetrahedron Lett.* **2015**, *56*, 3368-3372.
38. Stoychev, D., On the Role of Poly(Ethylene Glycol) in Deposition of Galvanic Copper Coatings. *Trans. IMF* **1998**, *76*, 73-80.
39. https://Rruff.Info/. (accessed 4/28/2022).
40. Wang, J.-P.; Cho, W.D., Oxidation Behavior of Pure Copper in Oxygen and/or Water Vapor at Intermediate Temperature. *ISIJ Int.* **2009**, *49*, 1926-1931.
41. Meng, F.; Jin, S., The Solution Growth of Copper Nanowires and Nanotubes Is Driven by Screw Dislocations. *Nano Lett.* **2012**, *12*, 234-239.
42. Lidiard, A., Thermodynamics and Kinetics of Point Defects. In Theory of Imperfect Crystalline Solids: Trieste Lectures 1970. Lectures Presented at an International Course, 1971.
43. Haugsrud, R.; Norby, T., Determination of Thermodynamics and Kinetics of Point Defects in Cu_2O Using the Rosenburg Method. *J. Electrochem. Soc.* **1999**, *146*, 999.
44. Xue, J.; Dieckmann, R., The Non-Stoichiometry and the Point Defect Structure of Cuprous Oxide ($Cu_{2-\delta}O$). *J. Phys. Chem. Solids* **1990**, *51*, 1263-1275.
45. Grzesik, Z.; Migdalska, M., Oxidation Mechanism of Cu_2O and Defect Structure of CuO at High Temperatures. *High Temp. Mater. Processes* **2011**, *30*, 277-287.
46. Kroger, F.A., *The Chemistry of Imperfect Crystals*; North-Holland Pub. Co.; Interscience Publishers: Amsterdam; New York, 1964.
47. Rahmel, A., High Temperature Corrosion. Von P. Kofstad. Elsevier Applied Science Publishers Ltd., London@ New York, 1988. 558 S., Zahlr. Abb. U. Tab., Preis: £ 68.00. *Mater. Corros. -Werkst. Und Korros.* **1988**, *39*, 354-354.
48. Biesinger, M.C.; Lau, L.W.; Gerson, A.R.; Smart, R.S.C., Resolving Surface Chemical States in XPS Analysis of First Row Transition Metals, Oxides and Hydroxides: Sc, Ti, V, Cu and Zn. *Appl. Surf. Sci.* **2010**, *257*, 887-898.
49. Biesinger, M.C., Advanced Analysis of Copper X-Ray Photoelectron Spectra. *Surf. Interface Anal.* **2017**, *49*, 1325-1334.
50. Jenkins, S.V.; Gohman, T.D.; Miller, E.K.; Chen, J., Synthesis of Hollow Gold–Silver Alloyed Nanoparticles: A "Galvanic Replacement" Experiment for Chemistry and Engineering Students. *J. Chem. Educ.* **2015**, *92*, 1056-1060.
51. Skrabalak, S.E.; Chen, J.; Sun, Y.; Lu, X.; Au, L.; Cobley, C.M.; Xia, Y., Gold Nanocages: Synthesis, Properties, and Applications. *Acc. Chem. Res.* **2008**, *41*, 1587-1595.
52. Kawabe, Y.; Ito, T.; Yoshida, H.; Moriwaki, H. Glowing Gold Nanoparticle Coating: Restoring the Lost Property from Bulk Gold. *Nanoscale*, 2019, *11*, 3786-3793.